Characterization and Application of Nanomaterials (2021) Volume 4 Issue 2
doi:10.24294/can.v4i2.1331

ORIGINAL RESEARCH ARTICLE

Electrospun $Li_3V_2(PO_4)_3$/carbon nanofiber as cathode materials for the high-performance lithium-ion batteries

Mengxi Zhao[1], Zhongpei Lu[1], Lin Chen[2], Xuefan Jiang[3], Fan Yin[1,2], Gang Yang[1,2*]

[1] *School of Chemistry and Material Engineering, Changshu Institute of Technology, Changshu 215500, Jiangsu, China. E-mail: gyang@cslg.cn*

[2] *School of Chemistry and Chemical Engineering, Jiangsu University, Zhenjiang 212013, Jiangsu, China*

[3] *School of Physics and Electronic Engineering, Changshu Institute of Technology, Changshu 215500, Jiangsu, China*

ABSTRACT

In this paper, a series of $Li_3V_2(PO_4)_3$/C composite nanofibers is prepared by a facile and environmentally friendly electrospinning method and calcined under different temperatures. The LVP nanofiber calcined under 900 °C exhibits the best electrochemical performance. The bicontinuous morphologies of LVP/CNF are the fibers shrunk and the LVP crystals simultaneously grown. At the range of 3.0–4.3 V, LVP/CNF obtained under 900 °C delivers the initial capacity of 135 mAh/g, close to the theoretical capacity of LVP. Even at high current density, the sample of LVP/CNF still presents good electrochemical performance.

Keywords: Lithium-ion Batteries; Cathode Material; Graphene; Nanocomposite; Electrochemical Performance

ARTICLE INFO

Received: 1 April 2021
Accepted: 20 May 2021
Available online: 28 May 2021

1. Introduction

Lithium battery has the advantages of high specific energy, high battery voltage, wide working temperature range and long storage life. It has been widely used in small electrical appliances, such as portable computers, cameras, electric tools, etc. In recent years, with the increasing shortage of non-renewable resources, such as oil and coal and the urgent needs of environmental protection, energy conservation and emission reduction, countries all over the world such as the United States, Japan Germany and France actively carry out the research on electric vehicle (EV) and hybrid electric vehicle (HEV), and put the development and application of lithium power battery on the important agenda. Because lithium battery has no pollution to the environment, it is more suitable to be used as the power supply of electric vehicle and large power reserve, so it has a very broad application prospect[1].

In recent years, great progress has been made in the research of positive and negative active materials for lithium batteries. At present, the most widely studied positive materials include layered lithium cobalt oxide $LiCoO_2$, spinel oxide $LiMn_2O_4$, phosphate $LiMPO_4$ (M = Mn, Fe, Co, etc.) and $Li_3V_2(PO_4)_3$, but these materials have their own shortcomings, It is difficult to meet the increasing requirements for lithium batteries[2–4]. Therefore, the existing electrode materials and search methods are improved. Finding new high-energy electrode materials is the top priority of research work, especially new cathode materials, which have become the key factor restricting the further improvement of the overall performance of Lithium batteries.

Monoclinic $Li_3V_2(PO_4)_3$ (LVP), as the cathode material of lithium-ion battery, has gradually attracted extensive attention because of its high theoretical capacity and energy density. The stable frame structure of LVP provides a three-dimensional channel for the insertion/removal of Li^+, and its theoretical capacity is as high as 197 mAh/g in the voltage range of 3.0–4.8 V[5–7]. However, the electronic conductivity of LVP is very poor. It affects the electrochemical performance of LVP and limits its commercial application. Researchers have proposed many methods to overcome the problem of electronic conductivity of LVP. In addition to effective carbon coating and metal ion doping, reducing the particle size or embedding LVP particles into carbon Nanonetworks can also effectively improve the electronic conductivity of LVP[8,9]. As we all know, the migration rate of ions and electrons in LVP plays a key role in improving its electrochemical properties. Therefore, it is a very effective method to improve both ionic conductivity and electronic conductivity, because nanostructured LVP is conducive to the movement and intercalation/de-intercalation of Li^+ in active electrode materials. It can improve the ionic conductivity of LVP. Conductive carbon materials can effectively improve the electronic conductivity of LVP. Nanostructured LVP/C materials can meet the requirements of high electronic and ionic conductivity at the same time. In recent years, LVP nanocomposites with different morphologies, such as spherical particles, nanorods, nanobelts, nanoplates and films, have attracted more and more attention. It is proved that it is beneficial to improve the electrochemical properties of LVP.

The preparation of nanofiber materials by electrospinning technology is a hot spot in the field of material science and technology in the world in recent ten years. Electrospinning has become the main way to effectively prepare nanofiber materials because of its simple manufacturing device, low spinning cost, wide variety of spinnable materials and controllable process. Electrospinning technology is a simple and low-cost method for preparing nanofibers, which has been widely used to prepare materials with one-dimensional nanostructures. With long length and porous structure, nanofibers obtained by electrospinning generally have a large specific surface volume ratio. Many nanofibers are randomly dispersed to form a multi space dense 3D structure. In recent years, the research on the preparation of olivine structure $LiMPO_4$ (M = Mn, Fe, Co, etc.) nanofibers by electrospinning is increasing, and the obtained $LiMPO_4$ fibers show good electrochemical properties[11–13]. However, there are few reports on the preparation of NASICON structure $Li_3V_2(PO_4)_3$. Considering that nanofibers are conducive to improvement. In this paper, $Li_3V_2(PO_4)_3$ with nanofiber structure was prepared by electrospinning, which improved the conductivity and electrochemical properties of $Li_3V_2(PO_4)_3$ as electrode material.

2. Experimental part

Firstly, electrospinning precursor was synthesized, an appropriate amount of citric acid was dissolved in deionized water, NH_4VO_3 and stoichiometric $NH_4H_2PO_3$ and $CH_3COOLi\cdot 2H_2O$ were added, and the reaction was stirred in oil bath for 4 h to obtain uniform mixed sol A. Polyvinylpyrrolidone (PVP) was added to an appropriate amount of H_2O and stirred for 4 h to obtain transparent viscous liquid B. Drop sol solution A into solution B and stir for 4 h to obtain uniform solution C. The precursor film is prepared by electrospinning method. The obtained white film is raised to 350 °C at a heating rate of 5 °C/min in nitrogen atmosphere and kept at a constant temperature for 4 h to decompose the mixture and release gas. Then it is cooled to room temperature with the furnace. After full grinding, it is burned in a high-temperature tubular furnace. In this process, PVP is carbonized. At the same time, lithium vanadium phosphate (LVP) is generated under high temperature. In order to study the optimal calcination temperature, the effects of heat treatment at four temperatures of 600 °C, 700 °C, 800 °C and 900 °C on the morphology and electrochemical properties of LVP/carbon nanofibers were tried.

The samples were analyzed by X-ray diffraction

(XRD) using D/max-2200/PC X-ray diffractometer of RIGAKU (Science) Company in Japan. The test conditions were Cu target, tube pressure 40 kV. The tube current is 100 Ma, the continuous scanning speed is 4°/min, and the step width is 0.02°. The sample surface morphology is analyzed by JSM-6700F scanning electron microscope produced by JEOL (Japan Electronics) Co., Ltd., the tube voltage is 10 kV and 15 kV, and the tube current is 10 μA.

The electrochemical performance test process of the sample is as follows: weigh the synthesized cathode material, conductive carbon black and polytetrafluoroethylene (PTFE) binder according to the mass percentage of 80:15:5, fully mix, and roll the material into 40 by manual membrane rolling machine μm thin film, cut into a square positive electrode sheet with a side length of 6 mm. The negative electrode adopts high-purity metal lithium sheet with a purity of 99.9%, a thickness of 0.4 mm and a diameter of 10 mm. In order to reduce the impact of humidity on the battery performance, the positive electrode sheet needs to be vacuum dried at 120 ^{o}C for 12 h before simulating the battery assembly. The battery assembly is carried out in a glove box filled with high-purity argon. The diaphragm used is Celgard 2500 microporous film, and the battery shell is 2016 button type. Place the positive shell, positive plate, diaphragm, negative plate and negative shell in order from top to bottom, and inject an appropriate amount of electrolyte. The solvent in the electrolyte is a 1:1:1 mixture of vinyl carbonate, diethyl carbonate and dimethyl carbonate, and the solute is $LiPF_6$. The charge discharge performance test of the assembled button battery with a concentration of 1 mol/l was carried out on the land CT2001A battery performance test system produced by Wuhan Lantian Electronics Co., Ltd.

3. Results and discussion

Figure 1 shows the surface morphology of the precursor of LVP/C composite nanofibers after drying in a 60 ^{o}C oven. It can be seen from **Figure 1(a)** that the fibers obtained by electrospinning are distributed continuously, and each fiber is interwoven vertically and horizontally to form a dense nanofiber film. However, it can be seen that the diameter distribution of the fibers is uneven. The fiber with larger diameter may be caused by the superposition of several fibers. **Figure 1(b)** shows the specific characteristics of the fiber more intuitively: the diameter is about 500 nm and the fiber surface is smooth.

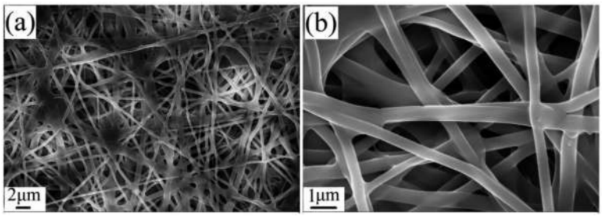

Figure 1. SEM image of the nanofiber precursors obtained from electrospinning.

The LVP nanofiber film obtained by electrospinning was treated at high temperature in a nitrogen atmosphere tubular furnace for 4 h. as shown in Figure 2, the SEM images after heat treatment at different temperatures. It can be seen from the figure that after high temperature treatment, the fibrous morphology of the precursor was not damaged, but different changes occurred on the basis of fiber dimension. However, temperature has a great influence on the morphology of the material. As shown in **Figure 2(a)** and **2(b)**, after calcination at 600 ^{o}C for 4 h, the fiber breaks, the diameter is about 600 nm, and small holes are formed on the fiber surface. Combined with XRD data analysis, we know that after calcination at 600 ^{o}C, no LVP phase is formed. Therefore, it can be judged that the fiber with rough surface shown in **Figures 2(a)** and **2(b)** is the carbon fiber obtained by PVP carbonization. After increasing the calcination temperature to 700 ^{o}C, the fiber surface changes significantly. As shown in **Figures 2(c)** and **2(d)**, the fiber does not break and the diameter becomes smaller at 600 ^{o}C, with improved continuity. In addition to similar pores, needle and block particles also appear on the fiber surface. It can be seen from the above analysis that the fiber is the carbide of PVP. Combined with the XRD analysis results, it can be inferred that the needle and block formed on the fiber surface should be the particles of LVP phase. When the temperature continues to rise to 800 ^{o}C, as shown in **Figure 2(e)** and **2(f)**, the diameter of the nanofibers obtained at 700 ^{o}C is close to that of the nanofibers, but the needles disappear, the number of massive particles gradually increases, distributed on the surface of the nanofibers, and the particle surface is smooth, which indicates that the LVP phase formed gradually increases with the increase of the calcination temperature. **Figure 2(g)** and **2(h)** are the SEM images after calcination for 4 h when the temperature rises to 900 °C, which can be clearly seen from the figure. The diameter of nanofibers is about 100 nm, and the LVP particles grow gradually. At this time, the PVP transformed carbon fibers still exist continuously and play a supporting role, and the LVP particles are distributed on its surface. It can be seen that the sintering temperature has an effect on the formation of LVP phase, and the heat treatment temperature affects the change of morphology in the treatment of electrospinning precursors.

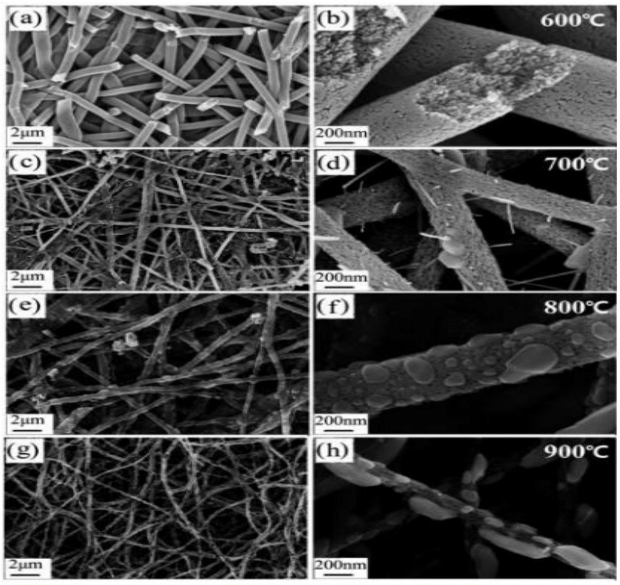

(a)(b):600 ℃;(c)(d):700 ℃;(e)(f):800 ℃;(g)(h):900 ℃

Figure 2. SEM profile of LVP at different calcination temperatures.

After high temperature treatment at different temperatures, the XRD diffraction patterns of each sample are shown in **Figure 3**. It can be seen from the figure that the XRD of the obtained LVP is obviously different. After high temperature treatment at 600 °C at the same heat treatment time, as shown in **Figure 3(a)**, there is no diffraction peak of LVP, showing amorphous characteristics. It shows that it is not enough to react at 600 °C to form LVP phase. When the heat treatment temperature rises to 700 °C, it can be clearly seen from **Figure 3(b)**, the XRD spectrum of the sample shows the characteristic diffraction peak of LVP, but the diffraction peaks of (002) and (111) crystal planes around 15° do not appear, indicating that the temperature still needs to be increased. When the temperature rises to 800 °C, as shown in **Figure 3(c)**. As shown in **Figure 3(d)**, in addition to the enhancement of the diffraction peak intensity, the diffraction peaks of (002) and (111) crystal planes also began to appear. **Figure 3(d)** shows the XRD diffraction peaks of LVP samples obtained after calcination for 4 h after the temperature increased to 900 °C, with monoclinic structure, belonging to P21/n space group, which corresponds to the standard spectral peaks one by one. From the analysis of XRD results, at the same time, Heat treatment temperature plays an important role in the formation of LVP phase.

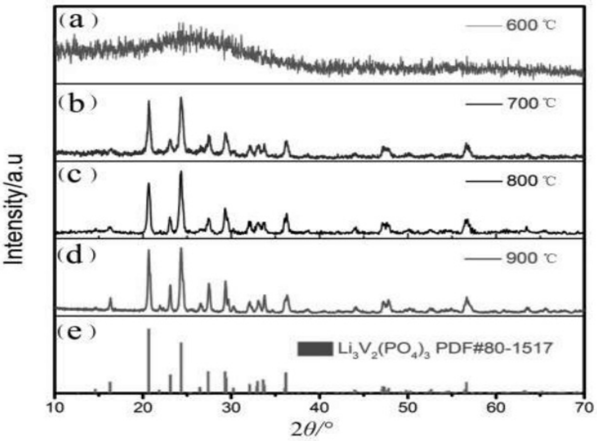

(a)600 ℃,(b)700 ℃,(c)800 ℃,(d)900 ℃

Figure 3. The XRD spectrogram of the LVP at the different calcination temperatures.

After high temperature heat treatment at 700 °C, 800 °C, 900 °C, the obtained LVP nanofibers were ground and prepared into electrode sheets, and then assembled into batteries. The electrochemical properties were tested respectively in the voltage range of 3.0–4.3 V and 3.0–4.8 V. **Figure 4** shows the constant magnification (0.1 C, 1 C = 133 MAH/g) of LVP samples in the voltage range of 3.0–4.3 V. It can be seen from the charging curve that there are three platforms at 3.59, 3.68 and 4.09 V, but these three platforms are not obvious for the LVP samples calcined at 700 °C and 800 °C, which is consistent with the XRD data because the crystallinity of LVP phase in the samples is not high. With the increase of temperature, the crystallinity of LVP phase gradually increases. The characteristic platform of LVP in the charge discharge curve is also gradually obvious. The cycle performance of each sample after 50 charge discharge cycles at a constant magnification of 0.1 C is shown in **Figure 4(b)**. It can be seen from the figure that with the increase of calcination temperature, the discharge specific capacity of LVP samples gradually increases, and the cycle stability also improves. After 50 cycles, specific discharge capacity of LVP at 900 °C, 800 °C, 700 °C retains 132 mAh/g, 119 mAh/g, and 92 mAh/g respectively, which are 90%, 91% and 76% of the initial discharge specific capacity respectively. According to the charge discharge test results at small magnification (0.1 C), the LVP samples treated at 700 °C have shown poor capacity and cycle stability. In order to further study the effect of 800 °C and 900 °C on the performance of LVP, the variable rate charge and discharge performance at high voltage was tested.

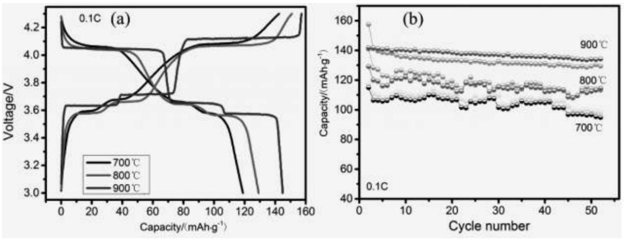

Figure 4. First circle charge and discharge curve and cycle performance diagram of the LVP in the 3.0–4.3 V voltage range obtained at different calcination temperatures, and the charge and discharge ratio is 0.1 C.

Figure 5 is the first charge discharge curve and cycle performance diagram of each electrode material under the charge discharge ratio of 0.1 C and 50 cycles in the voltage range of 3.0–4.8 V. When the battery is charged to 4.8 V, three Li^+ are completely separated from the LVP, with two-phase electrochemical platforms of 3.59, 3.68, 4.09 and 4.56 V respectively. The platforms of LVP charge curve obtained by calcination at 700 °C are not obvious, and in the discharge curve, the platforms of the three samples at about 4.0 V are inclined because of the irreversibility of the reaction. Two platforms can be seen in the discharge process, and the three discharge platforms are LVP electrodes. According to the cycle performance diagram in **Figure 5(b)**, the capacity of each sample decreases because the electrode material may dissolve in the electrolyte under high voltage, resulting in the instability of the LVP frame structure. After 50 cycles, the discharge specific capacities of the three samples are 114.2 mAh/g, 134.7 mAh/g, 151.6 mAh/g respectively, 74%, 73% and 77% of the specific discharge capacity of the first cycle are retained.

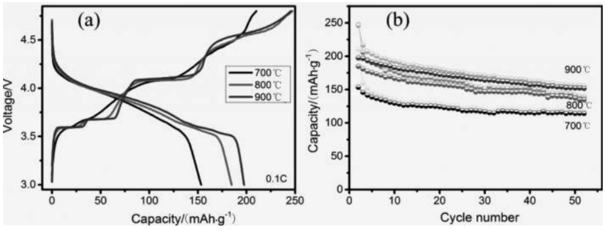

Figure 5. First cycle charge discharge curve and cycle performance diagram of LVP obtained at different calcination temperatures in the voltage range of 3.0–4.8 V. The charge discharge ratio is 0.1 C.

Similarly, we studied the variable rate performance of LVP samples calcined at 800 and 900 °C. As shown in **Figure 6**, the two samples were charged at constant current rate of 0.1 C and discharged at different discharge rates of 0.1 C, 1 C, 2 C, 5 C, 10 C and 20 C. It can be seen that with the increase of discharge ratio, the platform of charge discharge curve decreases gradually, and the first discharge specific capacity at each ratio decreases. LVP electrode calcined at 900 °C. Under the variable rate performance test, although the coulomb efficiency is less than 800 °C, the material shows good electrochemical performance. Even at higher rates, such as 10 C and 20 C, its specific discharge capacity can still maintain 88 mAh/g and 50 mAh/g. LVP nanoparticles are attached to carbon nanofibers with excellent conductivity. The composite structure effectively improves the electrochemical properties of LVP particles.

4. Conclusion

LVP nanofibers were prepared by a simple and feasible electrospinning method. LVP nanofibers with different morphologies were obtained after treatment at different calcination temperatures for

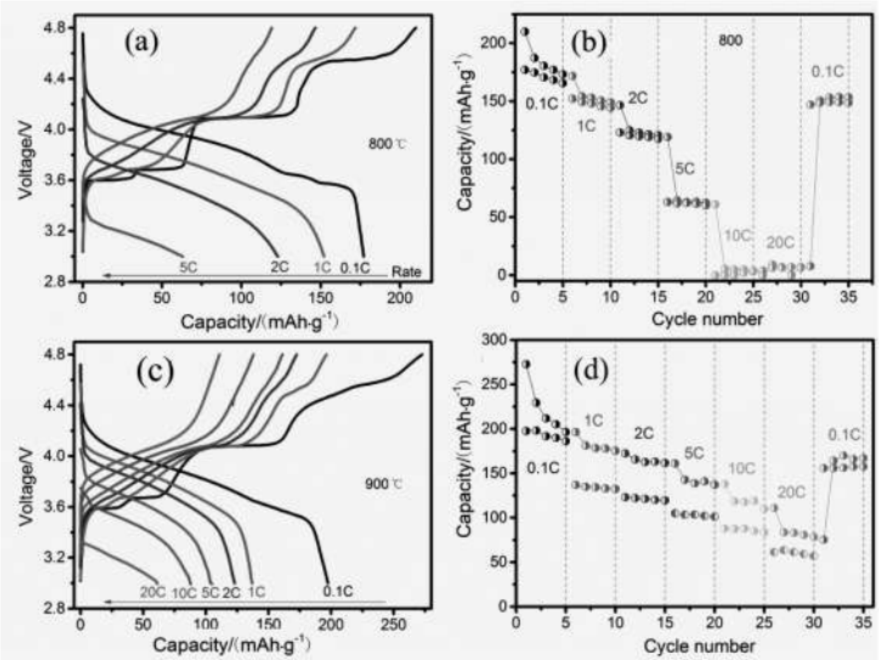

Figure 6. Magnification performance diagram of LVP/CNF obtained at 800 °C and 900 °C.

4 h. LVP particles can be embedded on the surface of nanofibers at higher temperatures. The sintering temperature plays an important role in the phase formation of LVP. The higher the temperature, the more LVP phase is formed, Through the test of electrochemical properties, the LVP calcined at 900 °C has good cycle performance and rate performance. Therefore, the LVP phase with high electrochemical activity is the most at this temperature. LVP nanoparticles are embedded on polymer fibers, and the particles are connected through fibers. Through comparison, the optimal sintering temperature is 900 °C. The first discharge capacities of LVP samples calcined at 800 °C and 900 °C are 134 mAh/g and 135 mAh/g in the voltage range of 3.0–4.3 V, reaching the theoretical capacity of $Li_3V_2(PO_4)_3$, which is 133 mAh/g. At high magnification, the LVP/C fiber composite sample still has excellent electrochemical properties.

Conflict of interest

The authors declare that they have no conflict of interest.

Acknowledgements

This work was supported by the Jiangsu Natural Science Foundation "Synthesis and Electrochemical Properties of Cathode Material Lithium Nickel Manganite of High Performance Lithium Batteries" (BK20141229).

References

1. Huang K, Wang Z, Liu S. Principle and key technology of lithium batteries (in Chinese). Beijing: Chemical Industry Press; 2007. p. 12.
2. Yang G, Liu H, Ji H, *et al.* Temperature-controlled microwave solid-state synthesis of $Li_3V_2(PO_4)_3$ as at cathode materials for lithium batteries. Journal of Power Sources 2010; 195: 5374–5378.
3. Zhang X, Wang K, Wei X, *et al.* Carbon-coated V_2O_5 Nanocrystals as high performance cathode materials for lithium ion batteries. Chemistry of Materials 2011; 23: 5290–5292.
4. Son J, Kim G, Kim M, *et al.* Carbon coated NASICON type $Li_3V_{2-x}M_x(PO_4)_3$ (M=Mn, Fe and Al) materials with enhanced cyclability for Li-ion batteries. Journal of the Electrochemical Society 2013; 160: A87–A92.
5. Sun C, Rajasekhara S, Dong Y, *et al.* Hydrothermal synthesis and electrochemical properties of $Li_3V_2(PO_4)_3$/C-based composites for Lithium batteries. ACS Applied Materials & Interfaces 2011; 3: 3772–3776.

6. Kuang Q, Zhao Y, Liang Z. Synthesis and electrochemical properties of Na-doped $Li_3V_2(PO_4)_3$ cathode materials for Li-ion batteries. Journal of Power Sources 2011; 196: 10169–10175.
7. Chen L, Yan B, Xu J, *et al.* Bicontinuous structure of $Li_3V_2(PO_4)_3$ clustered via carbon nanofiber as high-performance cathode material of Li-ion batteries. ACS Applied Materials & Interfaces 2015; 7: 13934–13943.
8. Liu H, Yang D, Zhang X, *et al.* Kinetics of conventional carbon coated-$Li_3V_2(PO_4)_3$ and nanocomposite $Li_3V_2(PO_4)_3$/graphene as cathode materials for power lithium ion batteries. Journal of Materials Chemistry 2012; 22: 11039–11048.
9. Wang H, Li Y, Huang C, *et al.* High-rate capability of $Li_3V_2(PO_4)_3$/C composites prepared via a polyvinylpyrrolidone-assisted sol-gel method. Journal of Power Sources 2012; 208: 282–287.
10. Yang Y, Wang H, Zhou Q, *et al.* Improved lithium storage properties of electrospun TiO_2 with tunable morphology: from porous anatase to necklace rutile. Nanoscale 2013; 5: 10267–10274.
11. Hagen RV, Lorrmann H, Moller KC, *et al.* Electrospun $LiFe_{1-y}Mn_yPO_4$/C Nanofiber Composites as Self-Supporting Cathodes in Li-ion batteries. Advanced Energy Materials 2012; 2: 553–559.
12. Damen L, Giorgio F D, Monaco S, *et al.* Synthesis and characterization of carbon-coated $LiMnPO_4$ and $LiMn_{1-x}Fe_xPO_4$ (x=0.2, 0.3) materials for lithium-ion batteries. Journal of Power Sources 2012; 218: 250–253.